Silver Nanoparticles Anchored 5-methoxy benzimidazol thiomethanol (MBITM): Modulate, Characterization and Comparative Studies on MBITM and Ag-MBITM Antibacterial Activities

IOP Conf. Series: Journal of Physics: Conf. Series **1294** (2019) 052026 doi:10.1088/1742-6596/1294/5/052026

Silver Nanoparticles Anchored 5-methoxy benzimidazol thiomethanol (MBITM): Modulate, Characterization and Comparative Studies on MBITM and Ag-MBITM Antibacterial Activities

Nuaman F Alheety [1], Abdulwahab H Majeed [2] and Mustafa A Alheety [3]

[1] Department of General Sciences, College of Basic Education, Al-Anbar University, Al-Anbar, Iraq.
[2] Department of Chemistry, College of Science, Diyala University, Diyala, Iraq.
[3] Department of Chemistry, College of Science, Tikrit University, Tikrit, Iraq.

e-mail : mustafa1990alheety@st.tu.edu.iq

Abstract. This research highlights the synthesis of novel organic molecule that is 5-methoxybenzimidazolthiomethanol (MBITM). This molecule is synthesized via the reaction of 5-Methoxy-2-mercaptobenzimidazole with formaldehyde in ethanol. This resulting molecule was characterized via Fourier-transform infrared spectroscopy (FTIR), proton-nuclear magnetic resonance (^{1}H-NMR) and elemental analysis (CHN). Furthermore, MBITM is used as a base compound for preparation of one novel nano material by mixing it with silver nanoparticles (Ag NPs) that prepared by green method using Zizyphus spina christi L (Seder) leaf, via a simple chemical reaction. The resulting Ag anchored MBITM (Ag-MBITM) was characterized by FTIR, X-ray diffraction (XRD) and Energy-dispersive X-ray spectroscopy (EDX) measurements. All these characterization measurements establish that a stable MBITM can be electrostatically retained on the surfaces of the Ag NPs. MBITM, Ag NPs and their nano derivative were screened for their antibacterial activity against both types of bacteria Gram-positive (S. aureus) and Gram-negative (E. Coli). In general, E-Coli and S. aureus were exposed to be significantly inhibited by all these three compounds but with different inhibition levels. Besides, the study of the biological activity was adopted for the purpose of conducting a comparative study between the raw materials (Ag NPs, MBITM) and the nanomaterial (Ag-MBITM) resulting from their reaction. The results showed that nanosilver-organic hybrid had effectively developed the antibacterial ability for both starting compounds. It has also been observed that this hybrid has been particularly effective with respect to the gram-positive bacteria.

Keywords: Silver nanoparticles; 5-methoxy-2-mercaptobenzimidazole; 5-methoxy benzimidazolethiomethanol; Antibacterial activity

1.Introduction

The discoveries of the antimicrobial agents are one of the most important discoveries in the history of pharmaceuticals. However, despite the industrial development of antibiotics, there are more than 800,000 cases of deaths annually due to some types of bacteria such as *S. aureus*, *P. aeroginosa* or

E.coli [1-3]. Microbes have the ability to resist drugs because they use different mechanisms for this purpose. For example, the microbes have the ability to produce enzymes that alter the chemical structure of the drugs used and can also induce a protein mutation so as to eliminate the toxic effect of these drugs on new genetically inherited bacteria furthermore bacteria sometimes limit the cell membrane 's permeability to the drug agent. [4]. As bacteria are resistant to these antibiotics, it is very important to afford an innovative way to address these challenges. Nanoscience provides a sophisticated platform for overcoming these challenges because nanomaterials circumvent some of the defects and constraints experienced by antimicrobial. This is because of the fact that nanoparticles are able to deliver the drug directly to the cell without the need to penetrate and thus overcome most drug resistance mechanisms [5]. In our study, silver nanoparticle was specifically selected for their transformation into organic-capped nanosilver because it has antimicrobial action against the bacteria [6-13] or fungi [14-16]. More importantly, it has no toxicity to human and animal cells [17-19]. For these reasons, silver nanoparticles are preferred to be used in the development of antibiotic. Many plant extracts were used to reduce the Ag^{+1} and convert it into the Ag^{0} nanoparticles [20-28]. Although there are many plants that have been used for this purpose, however in this research, the preparation of these nanoparticles was adopted using the extract of *Zizyphus spina christi L* leaf for many advantages such as no requirement for toxic solvent, economic, stability and compatibility [28]. During the survey in the published literature of Ag NPs toxicity, we could not determine the inhibition mechanism of bacteria. But we can conclude from the literature survey that the nanoparticle cause (i) either damage in the composition of protein or saccharide by binding to the amino or carboxylic terminal in the protein or hydroxyl in saccharides [29] or (ii) the occurrence of disorder or pitting in the cell membrane by generating reactive O_2 sorts [30-32]. It became apparent that the toxicity of the nanoparticle is mainly to its small size [29, 33], which qualifies it to enter the cells easily and is expected to undergo changes after entering different environments [34, 35]. From these observations, we conclude that it is important to pour attention on the surface/ coating agent. The choice of benzimidazole to inhibit the bacteria is due to the fact that these compounds are part of the composition of many pharmaceuticals [36] so it is important to study its effectiveness against bacteria. All previous studies have shown that benzimidazole derivatives have a mild effect against bacteria [37-41]. This is due to the inability of the benzimidazole base structure to penetrate the cell membranes [36]. Due to the resistance of the bacteria to this type of compounds, we decide to modify their chemical structure and then load it on the nanosilver to circumvent the bacteria and deliver this material to the cells directly and achieve the purpose of understanding the real effectiveness of these compounds.

2. Experimental part

2.1. Materials

Formaldehyde (CH_2O, 37.00%) and 5-Methoxy-2-mercaptobenzimidazole ($C_8H_8N_2OS$, 99.00%) are supplied from Fisher Scientific-ACROS Organics™, USA. Silver nitrate ($AgNO_3$, 99.99%), ethanol (C_2H_6O, 99%) and tri-sodium citrate dehydrate ($C_6H_9Na_3O_9$, ≥98%) are supplied by Sigma Aldrich Company, UK.

2.2. Instrumentations

All FTIR spectra were measured in PerkinElmer spectrophotometer (65 FT-IR) in a wave numbers (400-4000 cm^{-1}) as KBr discs. Elemental analysis of MBITM was carried on a CHN type Leco Truspec. ^{1}H- and $^{13}C\{^{1}H\}$ spectra of MBITM were measured by Varian Unity spectrometer (400 MHz) in d^6-DMSO solvent with internal standard ($(CH_3)_4Si$). XRD analysis of MBITM, Ag NPs and Ag-MBITM were performed using (ShemadzuXR6000) device with Ni-Cu filter (Cu Kα, λ = 1.5406 Å). EDXsof Ag NPs and Ag-MBITM were conducted using Oxford instruments SEM Tech.

2.3. Methods

2.3.1. Preparation of Zizyphus spina christi L aqueous extract: 25 g of fresh Seder leaf was washed five times with distilled water and thereafter cut into a small piece and immersed with 100 ml Millipore-Milli-Q water. This mixture was refluxed on a steam bath for 1 h and the resulted mixture was filtered off to give a bright yellow solution of Seder leaf aqueous extract.

2.3.2. Synthesis of silver nanoparticles (Ag NPs): This material was prepared according to the typical method described in [28]. Under dark conditions, 5 ml of 50% Seder aqueous extract was slowly added to approximately 180 ml of 1mM $AgNO_3$. This mixture was stirred at 30 ^oC to achieve a good mixing of the two components. After 35, the solution was turned from bright yellow to reddish brown then it centrifuged at 13500 rpm for 15 min. The obtained precipitate was purified by re-dispersed it in water five times.

2.3.3. Synthesis of 5-methoxybenzimidazolthiomethanol (MBITM): To (1.0000 g, 5.5000 mmol) of 5-methoxy-2-mercaptobenzimidazole in 35 ml of absolute ethanol, 5 ml of 37% formaldehyde was added drop wise under stirring. The resulting mixture was refluxed on a steam bath for 5 h and then evaporated near the dryness. The white solid was filtered, washed with cold ethanol and dried under vacuum. White solid, Yield: 1.050 g (90%). Anal. calc. for $C_9H_{10}N_2O_2S$: C, 51.41; H, 4.79; N, 13.32, Found, C, 51.50; H, 4.88; N, 13.39%. FTIR (KBr, cm^{-1}): 3393 υ(O–H); 3129 υ(N–H) 3030 υ(=C–H); 2958 υ(–C–H); 1628 υ(C=N); 1500 υ(C=C); 1361 υ(C–O–H); 650 υ(C–S). ^{1}H NMR (400 MHz, d^6-DMSO) δ 14.07 (s, 1H), 7.30 (dd, $J^3_{(H3-H4)}$= 8.8 and $J^4_{(H3-H1)}$= 2.0 Hz, 1H, H3), 7.07 (dd, $J^3_{(H4-H3)}$= 8.8 and $J^5_{(H4-H1)}$= 1.7 Hz, 1H, H4), 6.62 (d, $J^4_{(H1-H3)}$ = 2.0 Hz), 3.81 (s, 1H), 3.65 (s, 2H), 3.57 (s, 3H). Melting point: 125-128 ^oC. Numbering of atoms are illustrated in Scheme 1.

*2.3.4. Synthesis of Ag NPs Anchored MBITM (Ag-MBITM):*This nano material was prepared by the direct addition of the (0.1000 g, 0.4756 mmol) MBITM solution in 5 ml of hot ethanol to the (0.0256 g, 0.2375 mmol) silver nanoparticle in 50 ml deionized water. This mixture was first mixed and reacted by sonication device for 1 h and then refluxed for 1 h. The resultant mixture was left cold at laboratory temperature and centrifuged at 13000 rpm for 10 min. The precipitate was dispersed again in ethanol and centrifuged again to remove unreacted MBITM. The Ag NPs Anchored MBITM was stored in de-ionized water 0.06 g in 20 ml for further steps.

2.3.5. Antibacterial Assay

The antimicrobial activity of prepared MBITM, Ag NPs and Ag-MBITM were assessed against S. aureus and E. coli cultured on the plates of Mueller Hinton Agar by a well diffusion method [27].

3. Results and discussions

3.1. Synthesis and characterization of 5-methoxybenzimidazolthiomethanol

The preparation of the MBITM was carried out by reaction the formaldehyde with 5-Methoxy-2-mercaptobenzimidazole in ethanol as in the Scheme 1.

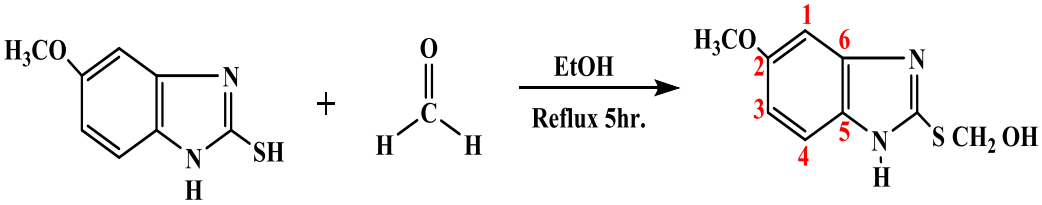

Scheme 1: Chemical equation for preparation of MBITM

Despite the acidity of both protons of the NH and SH groups, however, the results of the measurements showed that the reaction was obtained with a proton of the SH group. This is because the acidity of the proton associated with SH is more than that associated with NH**.** Accordingly, the proposed mechanical shall be as in Scheme 2.

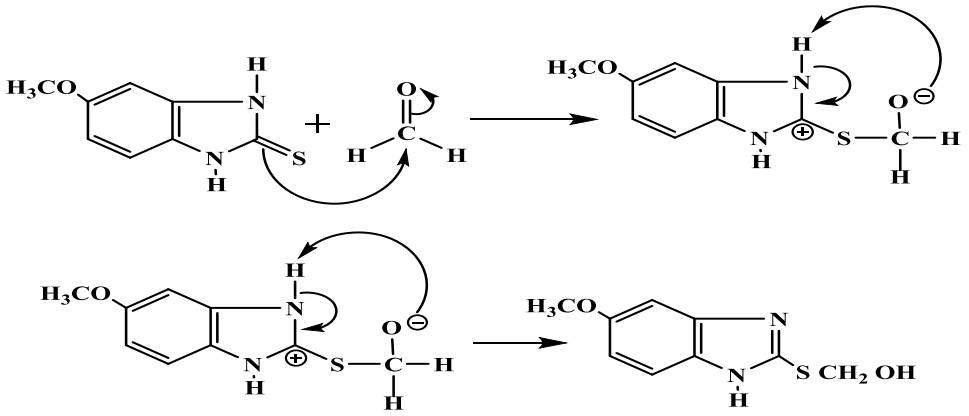

Scheme 2: The proposed mechanism for the formation of MBITM

The structure of MBITM was firstly characterized by FTIR spectrum (Figure 1). The spectrum shows the following main peaks: 3393, 3129, 3030, 2968, 1361 and 650 cm^{-1}, represent the ν(OH), ν(N-H), ν(=C-H), ν(CH_2), ν(C-O-H) and ν(C-S), respectively. Besides, the presence of the new peaks of ν(OH) and ν(CH_2) are fully demonstrating the proposed structure. The ^{1}H-NMR spectrum (Figure 2) showed good separation for the signals, where the three signals of the aromatic ring showed a doublet of doublet signal of 1H3 at 7.30 ppm with a value of $J^3_{(H3\text{-}H4)}$= 8.8 and $J^4_{(H3\text{-}H1)}$= 2.0 Hz. Another doublet of doublet signal of 1H4 at 7.07 ppm with a value of $J^3_{(H4\text{-}H3)}$= 8.8 and $J^5_{(H4\text{-}H1)}$= 1.7 Hz. The 1H1 proton signal appeared as a doublet signal at 6.61ppm with $J^4_{(H1\text{-}H3)}$ = 2.0Hz. Depending on the values of the coupling constant, the chemical shift of each proton was determined. This is due to the fact that J values are inversely proportional to the distance between the protons. The spectrum also showed four single signals at 14.07, 3.81, 3.65 and 3.57 ppm, attributed to the proton of NH, OH, CH_2 and CH_3, respectively. In order to prove the structure doubly, the measurement of the elemental analysis was performed. The results showed a very large correlation between the theoretical and practical values of the proposed formula as described in 2.3.3. The measurement of the melting point was very beneficial because there was a significant difference of 120 ° C between the starting material (248- 249) and the resulting material (125- 128), which is evidence of a change in structure.

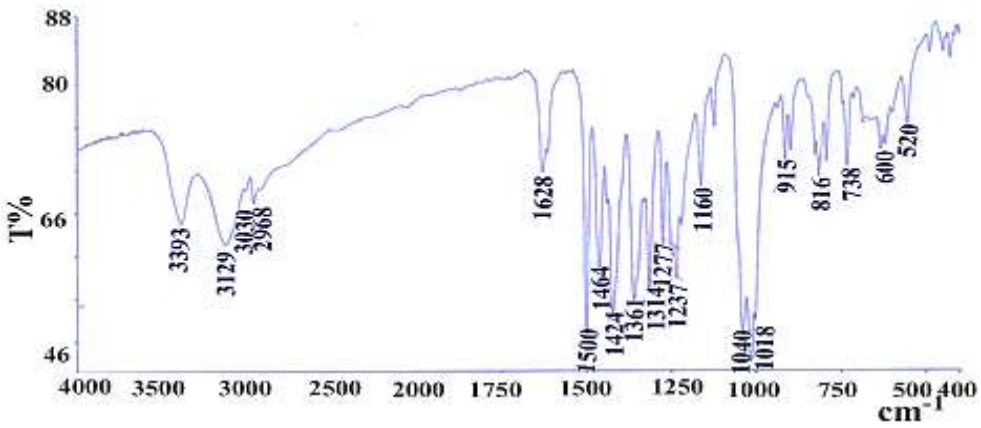

Figure 1: FTIR spectrum of MBITM

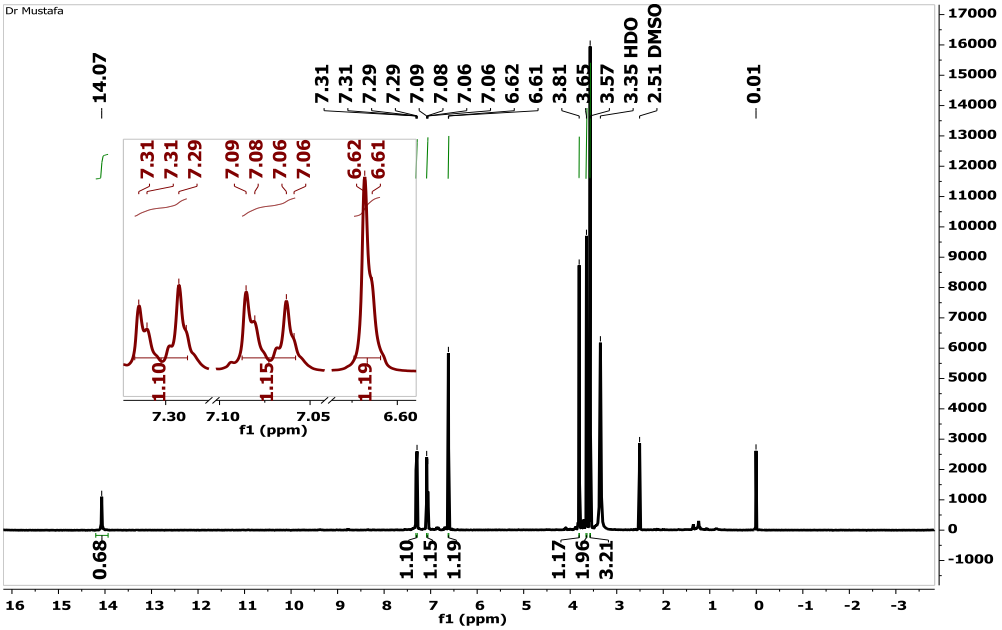

Figure 2: ^{1}H-NMR spectrum of MBITM

3.2. Characterization of Ag NPs and Ag NPs anchored MBITM

3.2.1. FTIR: The FTIR spectrum of Ag NPs (Figure 3) revealed the presence of ν(O–H) at 3445 cm^{-1}, ν(-C–H) of aliphatic content at 2975 cm^{-1}, ν(C=C) at 1605 cm^{-1}, ν(C-O) at 1350 cm^{-1} and the bands of aromatic substituted at 775 and 710 cm^{-1}. These bands are attributed to aromatic substituted of the adsorbed components from the seder extract. These bands strongly demonstrate the presence of terpenoids [42,43].

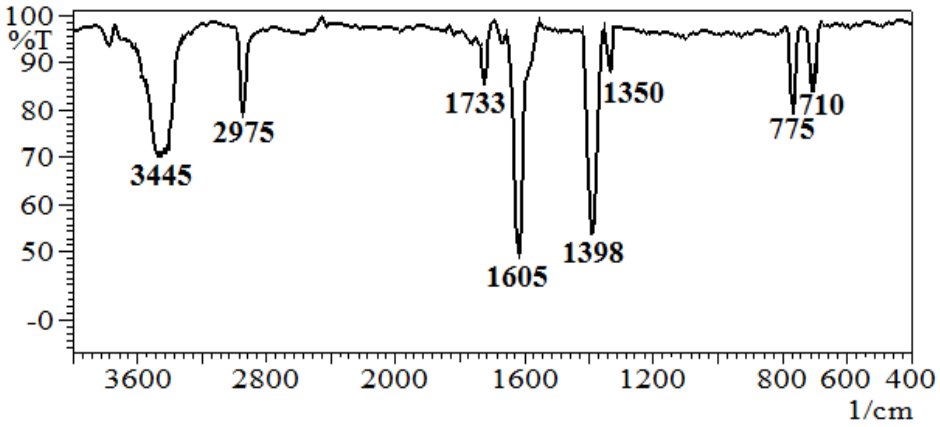

Figure 3: FTIR spectrum of Ag NPs

In the case of the FTIR spectrum of Ag-MBITM (Figure 4), the spectrum shows that the ν(OH) at 3380 and ν(C-O-H) at 1338 is shifted to lower frequencies than that in the FTIR of analog MBITM (1037, 1431 cm^{-1}) after the addition of Ag nanoparticles indicating the association of the MBITM through the hydroxy terminal.

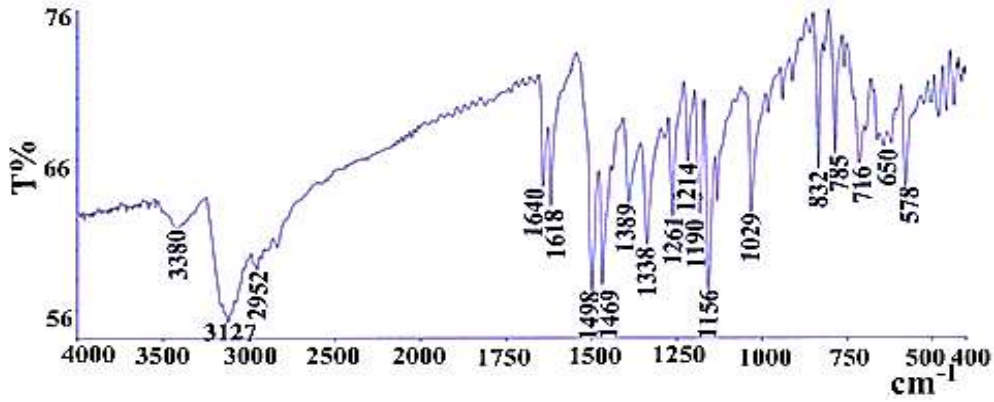

Figure 4: FTIR spectrum of Ag-MBITM

3.2.2. *XRD*: The XRD pattern for the Ag NPs and Ag-MBITM were studied in order to check the difference in the XRD patterns of the Ag NPs and its derivative. In XRD pattern of the Ag NPs (Figure 5 (a)) there are four main peaks identified at (2θ) 38.2408°, ٤٤.٤٢٣٥°, ٦٤.٥٩٠٣° and 77.5154° corresponding to the (1 1 1), (2 0 0), (2 2 0) and (3 1 1) planes respectively [16] which are indexed to the face centered cubic system. The calculations of the particle sizes were illustrated in Table 1. As shown in Figure 5 (b), the XRD pattern Ag-MBITM shows that there were several main peaks listed in Table 1. It is worth focusing on the presence of the peaks of silver nanoparticles at 37.8155°, 64.5429° and 78.6089° with a slight shift in the values of 2 theta. The existence of these peaks clearly confirms that nanosilver is present in the Ag-MBITM composition. In addition, the existence of other peaks due to organic matter is another proof of the Ag-MBITM being prepared. Using the Debye-Scherrer equation [44], the crystallite size of the Ag NPs and Ag-MBITM were determined. The calculation results show that the average size of Ag NPs was 22.07 nm while it was 13.59 nm regarding to Ag-MBITM. It can easily be observed that the average size decreased with the addition of MBITM.

Table 1: X-ray diffraction information for prepared compounds and average size of nanoparticles

Compound	Peak no.	2θ (degree)	d-spacing (A^0)	FWHM (degree)	D (nm)	D average (nm)
Ag NPs	1	٣٨.٢٤٠٨	٢.٣٥١٦٧	٠.٤٢٧٣٠	20.56	22.07
	2	٤٤.٤٢٣٥	٢.٠٣٧٦٧	٠.٤٩١٥٠	18.24	
	3	٦٤.٥٩٠٣	2.12300	٠.٤١٠٥٠	23.92	
	4	٧٧.٥١٥٤	١.٤٤١٧٥	٠.٤١٦٤٠	25.57	
Ag-MBITM	1	13.5647	٦.٥٢٢٥٤	٠.٦٩٠٠٠	12.11	13.59
	2	20.7099	٤.٢٨٥٥٠	٠.٤٤٨٣٠	18.82	
	3	24.1193	٣.٦٨٦٨٨	٠.٤٨٣٠٠	17.57	
	4	26.5167	٣.٣٥٨٧٤	٠.٨٣٦٧٠	10.19	
	5	27.7630	٣.٢١٠٧٣	٠.٥٢٦٧٠	16.23	
	6	٣٣.٧٦٠٧	٢.٦٥٢٧٩	٠.٧٣٦٧٠	11.77	
	7	٣٧.٨١٥٥	٢.٣٧٧١٤	٠.٨٠٠٠٠	10.97	
	8	٥١.٦٦٠٠	١.٧٦٧٩٥	٠.٨٥٥٠٠	10.79	
	9	٦٤.٥٤٢٩	١.٤٤٢٧٠	٠.٦٨٠٠٠	14.44	
	10	٧٨.٦٠٨٩	١.٢١٦٠٦	٠.٨٢٠٠٠	13.08	

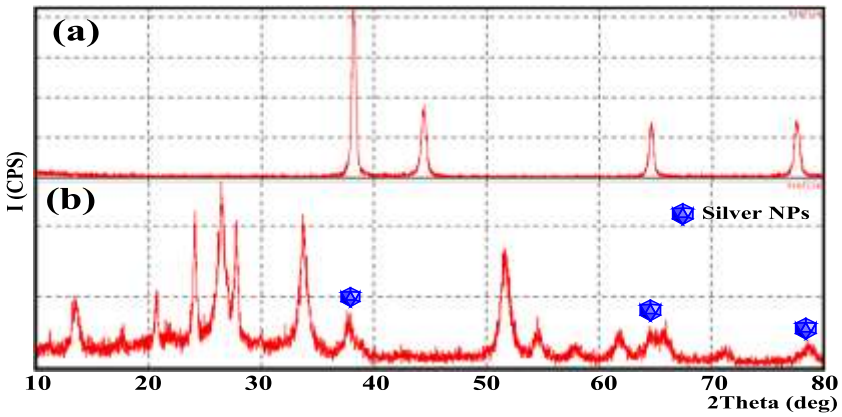

Figure 5: XRD patterns of (a) Ag NPs and (b) Ag-MBITM

3.2.3. EDX : The EDX of pure Ag NPs (Figure 6 (a)) showed the presence of silver signal at 2.98 KeV only. The existence of this signal alone is evidence of the purity of the prepared Ag NPs. In the case of Ag-MBITM, in addition to silver signal at 2.98 KeV, the EDX showed the carbon signal at 0.27 keV, oxygen at 0.52 KeV and sulfur signal at 2.30 KeV as shown in Figure 6 (b). The existence of a sulfur signal of the exocyclic sulfur in the MBITM, is conclusive evidence of the success of the reaction between Ag NPs and MBITM.

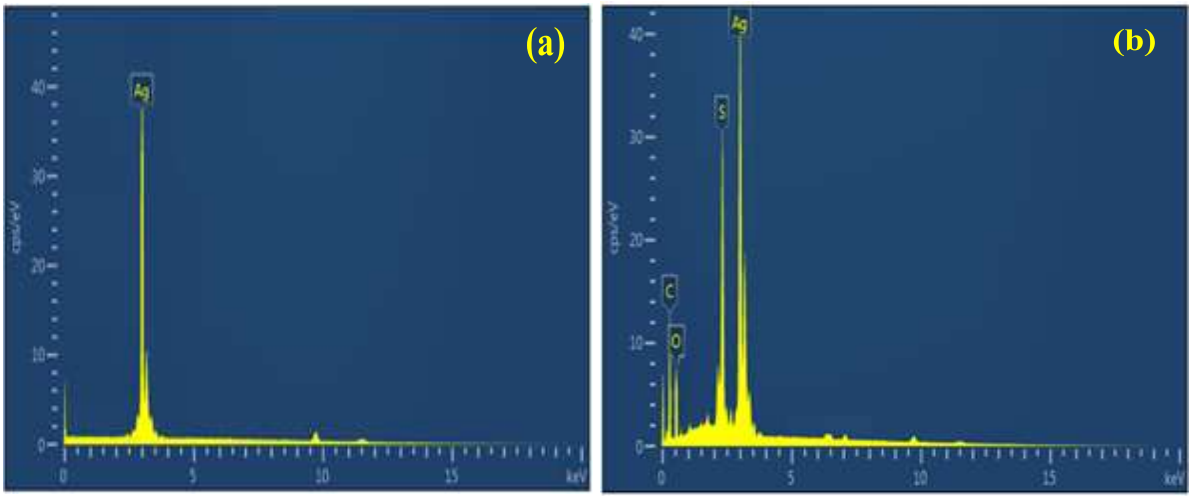

Figure 6: EDX patterns of (a) Ag NPs and (b) Ag-MBITM

3.2.4. Antibacterial activity: E. coli and S. aureus bacteria were subjected to two different concentrations (2 mM, 4 mM) of AgNPs, MBITM and Ag-MBITM samples. The inhibition zone diameter (IZD) in mm is shown in Table 1. The results of the anti-bacterial activities proved that all the prepared materials were able to kill both types of bacteria (Gram-positive and Gram-negative) as well as the results proved that by increasing the concentration of the antibacterial agents, the toxicity increases and thus increase the IZD. AgNPs exhibits a relatively greater IZD against the S.aureus, while for MBITM there was no significant difference in IZD against both types of bacteria. As for the nano-organic hybrid (Ag-MBITM), compared to the two pure starting materials, it had a more than double effect. This multiplier effect is due to the ability of the AgNPs to transfer the

functionalized benzimidazole derivative to the bacterial cells due to the small size of the nanoparticles, which was confirmed by the X- ray measurements, since the addition of the benzimidazole derivative led to a significant reduction in the size of the Ag- MBITM particles compared to the AgNPs.

Table 2 Antibacterial activity test of the prepared materials

Antibacterial agent	IZD (mm) after incubation for 24 hr	
	E. coli	S. aureus
AgNPs /2mM	2.01	2.40
AgNPs /4mM	5.04	5.70
MBITM/2mM	3.26	3.01
MBITM/4mM	6.41	6.97
Ag-MBITM/2mM	8.22	10.10
Ag-MBITM/4mM	14.65	17.39

4. Conclusion

This article presents the preparation and characterization of new organic material (MBITM) as well as includes the preparation of silver nanoparticles using a green chemistry method, including the use of seder leaf extract as a reducing agent. In addition, this organic compound was anchored onto Ag nanoparticles, yielding in an Ag-MBITM compound, which was diagnosed with different techniques. The average particle size calculated by the Debye-Scherrer equation proved that Ag-MBITM is smaller than Ag NPs alone. This indicates that the silver clusters are separated by MBITM. The results of antibacterial measurements have shown that the combination of this organic compound with nanoparticles has improved the bio-activity properties of both pure silver and organic compounds. This information proves that silver has delivered organic matter into cells more easily through its ability to circumvent antibiotic resistance mechanisms. Now, we can demonstrate that the benzimidazole family has a strong anti-bacterial effect but need to find a way to deliver it directly to the bacteria cells. Therefore, we recommend preparing pharmaceutical products based on the presence of benzimidazole attached to nanoparticles.

5. References

[1] Jadali F, Karimi A, Fallah F, Zahraei M, Esteghamati A,Navidinia M, et al. 2013 A survey on Rotavirus Associated Diarrhea in 5 Main Cities of Iran *Arch Pediatr Infect Dis.***1** 23-6.

[2] Eslami G, Fallah F, Taheri S, Navidinia M, Dabiri H, Dadashi M et al 2013 Evaluation of antibacterial effect of cinnamon extract on Helicobacter pylori isolated from dyspeptic patients *Research in Medicine* **2** 85-9

[3] Goudarzi M 1 , Seyedjavadi SS , Fazeli M , Roshani M , Azad M , Heidary M , Navidinia M and Goudarzi H 2016 Identification of a Novel Cassette Array in Integronbearing Helicobacter Pylori Strains Isolated from Iranian Patients *Asian Pacific Journal of Cancer Prevention* **7** 309-15.

[4] Alekshun M N and Levy S B 2007 Molecular mechanisms of antibacterial multidrug resistance *Cell* **128**.

[5] Beyth N, Houri-Haddad Y, Domb A, Khan W and Hazan R 2015 Alternative antimicrobial approach: nano-antimicrobial materials. *Evid. Based Comp.l Altern. Med*. **16**.

[6] Pawar H V, Tetteh J, Debrah P and Boateng J S 2019 Comparison of in vitro antibacterial activity of streptomycin-diclofenac loaded composite biomaterial dressings with commercial silver based antimicrobial wound dressings *International journal of biological macromolecules* **121** 191-9.

[7] Roy S, Shankar S, and Rhim J W 2019 Melanin-mediated synthesis of silver nanoparticle and its use for the preparation of carrageenan-based antibacterial films *Food Hydrocolloids* **88** 237-46.
[8] Brobbey K J, Haapanen J, Mäkelä J M, Gunell M, Eerola E, Rosqvist E and Toivakka, M 2019 Effect of plasma coating on antibacterial activity of silver nanoparticles *Thin Solid Films* **672** 75-82.
[9] Naeem H, Ajmal ., Qureshi R B, Muntha S T, Farooq M and Siddiq M 2019 Facile synthesis of graphene oxide–silver nanocomposite for decontamination of water from multiple pollutants by adsorption, catalysis and antibacterial activity *Journal of environmental management* **230** 199-211.
[10] Rolim W R, Pelegrino M T, Lima A B, Ferraz L S, Costa F N, Bernardes J S and Seabra A B 2019 Green tea extract mediated biogenic synthesis of silver nanoparticles: Characterization, cytotoxicity evaluation and antibacterial activity *Applied Surface Science* **463** 66-74.
[11] Surwade P, Ghildyal C, Weikel C, Luxton T, Peloquin D, Fan X and Shah V 2019 Augmented antibacterial activity of ampicillin with silver nanoparticles against methicillin-resistant Staphylococcus aureus (MRSA) *The Journal of antibiotics* **72 50-3**.
[12] Zhang X, Wang W and Yu D 2018 Synthesis of waterborne polyurethane–silver nanoparticle antibacterial coating for synthetic leather *Journal of Coatings Technology and Research* **15** 415-23.
[13] Chen H, Zhao X, Liu Y, Kong F and Ji X 2018 Facile synthesis of elemental silver by the seed nucleus embedding method for antibacterial applications *Cellulose* **9** 5289-96.
[14] Meran Z, Besinis A, De Peralta T and Handy R D 2018 Antifungal properties and biocompatibility of silver nanoparticle coatings on silicone maxillofacial prostheses in vitro *Journal of Biomedical Materials Research Part B: Applied Biomaterials* **3** 1038-51.
[15] Bocate K P, Reis G F, de Souza P C, Junior A G O, Durán N, Nakazato G and Panagio L A 2019 Antifungal activity of silver nanoparticles and simvastatin against toxigenic species of Aspergillus *International journal of food microbiology* **291** 79-86.
[16] Alheety M A and Hameed A A 2018 Synthesis, characterization and antifungal activity of coated silver nanoparticles-nystatin and coated silver nanoparticles-clotrimazol. Tikrit *Journal of Pure Science* **7** 63-70.
[17] Bonilla J J A, Guerrero D J P, Saez R G T, Ishida K, Fonseca B B, Rozental S, Lopez C C O 2017 Green synthesis of silver nanoparticles using maltose and cysteine and their effect on cell wall envelope shapes and microbial growth of Candida spp. *Nanosci. Nanotechnol*. **17** 1729-39.
[18] Patra J K and Baek K H 2017 Antibacterial activity and synergistic antibacterial potential of biosynthesized silver nanoparticles against foodborne pathogenic bacteria along with its anticandidal and antioxidant effects *Front Microbiol* **8** 167-181.
[19] Agnihotri S, Mukherji S and Mukherji S 2014 Size-controlled silver nanoparticles synthesized over the range 5e100 nm using the same protocol and their antibacterial efficacy *RSC Adv*. **4** 3974-83.
[20] Renganathanet al 2014 synthesis and caracterization of silver nanoparticles fromErythrina Indica *Asian J. Pharm. Clin. Res.* **7** 39-43.
[21] Sumitha S, Vasanthi S, Shalini S, Chinni S V, Gopinath S C B, Kathiresan S and Ravichandran V 2019 Durio zibethinus rind extract mediated green synthesis of silver nanoparticles: Characterization and biomedical applications *Pharmacognosy Magazine* **60** 52-8.
[22] Ramar K, Gnanamoorthy G, Mukundan D, Vasanthakumari R, Narayanan V and Ahamed A J 2019 Environmental and antimicrobial properties of silver nanoparticles synthesized using Azadirachta indica Juss leaves extract *SN Applied Sciences* **1** 128.
[23] Onitsuka S, Hamada T and Okamura H 2019 Preparation of antimicrobial gold and silver nanoparticles from tea leaf extracts *Colloids and Surfaces B: Biointerfaces* **173** 242-48.
[24] Fatema S, Shirsat M, Farooqui M and Pathan M A 2019 Biosynthesis of Silver nanoparticle

using aqueous extract of Saraca asoca leaves, its characterization and antimicrobial activity *International Journal of Nano Dimension* **2** 163-68.

[25] Anbu P, Gopinath S C, Yun H S and Lee C G 2019 Temperature-dependent green biosynthesis and characterization of silver nanoparticles using balloon flower plants and their antibacterial potential *Journal of Molecular Structure* **1177** 302-09.

[26] Khoshnamvand M, Huo C and Liu J 2019 Silver nanoparticles synthesized using Allium ampeloprasum L. leaf extract: Characterization and performance in catalytic reduction of 4-nitrophenol and antioxidant activity *Journal of Molecular Structure* **1175** 90-6.

[27] Chellakannu M, Panneerselvam T and Rajeshkumar S 2019 Kinetic study on the herbal synthesis of silver nanoparticles and its antioxi-dant and antibacterial effect against gastrointestinal pathogens *International Journal of Research in Pharmaceutical Sciences* **10** 407-14.

[28] Halawani E M 2017 Rapid Biosynthesis Method and Characterization of Silver Nanoparticles Using Zizyphus spina christi Leaf Extract and Their Antibacterial Efficacy in Therapeutic Application *Journal of Biomaterials and Nanobiotechnology* **8** 22-35.

[29] Mapara N, Sharma M, Shriram V, Bharadwaj R, Mohite K C and Kumar V 2015 Antimicrobial potentials ofHelicteres isorasilver nanoparticles against extensively drug-resistant (XDR) clinical isolates of Pseudomonas aeruginosa *Appl. Microbiol. Biotechnol.* **99** 10655-67.

[30] Choi O and Hu Z Q 2008 Size dependent and reactive oxygen species related nanosilver toxicity to nitrifying bacteria *Environ. Sci. Technol*. **42** 4583–8

[31] El Badawy A M, Silva R G, Morris B, Scheckel K G, Suidan MT and Tolaymat TM 2011 Surface charge-dependent toxicity of silver nanoparticles *Environ. Sci. Technol*. **45** 283–7.

[32] Fabrega J, Renshaw J C, Lead J R 2009 Interactions of silver nanoparticles with Pseudomonas putidabiofilms *Environ. Sci. Technol*. **43** 9004–9.

[33] Park M V, Neigh A M, Vermeulen J P, de la Fonteyne L J, Verharen H W, Briedé J J, et al 2011 The effect of particle size on the cytotoxicity, inflammation, developmental toxicity and genotoxicity of silver nanoparticles *Biomaterials* **36** 9810–7.

[34] Tejamaya M, Römer I, Merrifield R C and Lead J R 2012 Stability of citrate, PVP, and PEG coated silver nanoparticles in ecotoxicology media *Environ. Sci. Technol.***13** 7011–7.

[35] Lowry G V, Gregory K B, Apte S C, Lead J R 2012 Transformation of nanomaterials in the environment *Environ. Sci. Technol.* **46** 6893–9.

[36] Negi D S, Kumar G, Singh M and Singh N 2017 Antibacterial Activity of Benzimidazole Derivatives: A Mini Review *Research & Reviews: Journal of Chemistry* **3** 18-28.

[37] Krim K et al 2012 Efficient microwave-assisted synthesis, antibacterial activity and high fluorescence of 5 benzimidazolyl-2′-deoxyuridines *Bioorganic & medicinal chemistry* **20** 480-86.

[38] Moreira M et al 2013 Antibacterial activity of head-to-head bis-benzimidazoles *International journal of antimicrobial agents* **42** 361-6.

[39] Al-Mohammed et al 2013 Synthesis and antibacterial evaluation of some novel imidazole and benzimidazole sulfonamides *Molecules* **18** 11978-95.

[40] Desai N C et al 2014 Synthesis, antibacterial and antitubercular activities of benzimidazole bearing substituted 2-pyridone motifs *European journal of medicinal chemistry* **82** 480-9.

[41] Noolvi N et al 2014 Synthesis, antimicrobial andcytotoxic activity of novel azetidine-2-one derivatives of 1H-benzimidazole *Arabian Journal of Chemistry* **7** 219-26.

[42] Jyoti K, Baunthiya M and Singh A 2016 *J. Radiat. Res. Appl. Sci.* **9** 217-27.

[43] Prakash P, Gnanaprakasam P, Emmanuel R, Arokiyaraj S and Saravanan M 2013 *Colloids Surf. B Biointerfaces* **108** 255-9.

[44] Jebour I K, Mohammed M Y and Alheety M A 2016 Synthesis and Characterization of Novel Nano Dithiocarbamate Complexes Derived From GO-benzimidazole *Diyala Journal For Pure Science* **1** 108-21.